Scanning Microscopy

Volume 8 | Number 3 Article 8

9-20-1994

A New Atomic Force Microscopy Technique for the Measurement of the Elastic Properties of Biological Materials

W. Xu
Dalhousie University

P. J. Mulhern
Dalhousie University

B. L. Blackford
Dalhousie University

M. H. Jericho
Dalhousie University, jericho@ac.dal.ca

I. Templeton
Institute for Microstructural Sciences, Ottawa

Scanning Microscopy, Vol. 8, No. 3, 1994 (Pages 499-506) 0891-7035/94$5.00+.25
Scanning Microscopy International, Chicago (AMF O'Hare), IL 60666 USA

A NEW ATOMIC FORCE MICROSCOPY TECHNIQUE FOR THE MEASUREMENT OF THE ELASTIC PROPERTIES OF BIOLOGICAL MATERIALS

W. Xu, P.J. Mulhern, B.L. Blackford, M.H. Jericho*, and I. Templeton[1]

Physics Department, Dalhousie University, Halifax, Nova Scotia, Canada B3H 3J5
[1]Institute for Microstructural Sciences, Ottawa, Ontario, Canada K1A 0R6

(Received for publication May 11, 1994 and in revised form September 20, 1994)

Abstract

We developed a new technique to measure elastic properties by using the atomic force microscope (AFM) tip to press samples into grooves etched in a GaAs substrate.

We measured the Young's modulus of β-chitin fibres with cross-sections less than 40 nm X 20 nm to be 1-2 X 10^{11} N/m^2. In the isotropic approximation, the Young's modulus of the S-layer sheath of the archaeobacterium *Methanospirillum hungatei* was 1-3 X 10^{10} N/m^2. By testing the sheath to breaking strength we estimated the bacterium can sustain an internal pressure as high as 100-200 atmospheres (1-2 x 10^7 N/m^2).

Key Words: Atomic force microscopy (AFM), force, elasticity, chitin, *Methanospirillum hungatei*, internal pressure.

*Address for Correspondence:
M. H. Jericho
Dalhousie University
Department of Physics
Halifax, NS B3H 3J5 Canada
Telephone number: 902 494 2316
FAX number: 902 494 5191
E-Mail: JERICHO@AC.DAL.CA

Introduction

Cell biology and nanotechnology are creating new interest in the properties of materials on the microscopic rather than the macroscopic scale. The elastic properties of materials on a nanometer scale are of particular interest since they can, for example, determine to what extent applied stress and strain modulate the morphology and metabolism of a cell (Tran-Son-Tay, 1993). However, macroscopic objects are often composite materials and the behaviour of the individual components is critical to understanding the properties at the molecular level.

Very few techniques exist that can measure elastic properties on the cellular or sub-cellular levels. The elastic moduli and viscosity of red blood cell membranes were measured with an area dilation method based on the micropipet (Evans *et al.*, 1976). Weisenhorn *et al.* (1993a,b) used the atomic force mic oscope (AFM) and an indentation method to measure the Young's modulus of cartilage and living cells.

We present an alternative AFM technique for probing the elastic properties of biological materials. Our technique involves pressing on the centre of a sample spanning a gap, and measuring the free deflection into the gap. This technique does not require the material to be softer than the substrate, and can be applied to anisotropic materials.

We illustrate this technique with a discussion of the elastic properties of chitin from *Thalassiosira fluviatilis* and the outer sheath of *Methanospirillum hungatei*. Suitable models not only provide information on the Young's modulus, but also can give insight into possible biological mechanisms.

Measurement Technique

Our technique assumes that there is a way of supporting the material of interest so that a length of it does not rest on the substrate. Initially, we prepared a mat of chitin fibres and measured those fibres that were supported on others (Jericho *et al.*, 1993), but this tech-

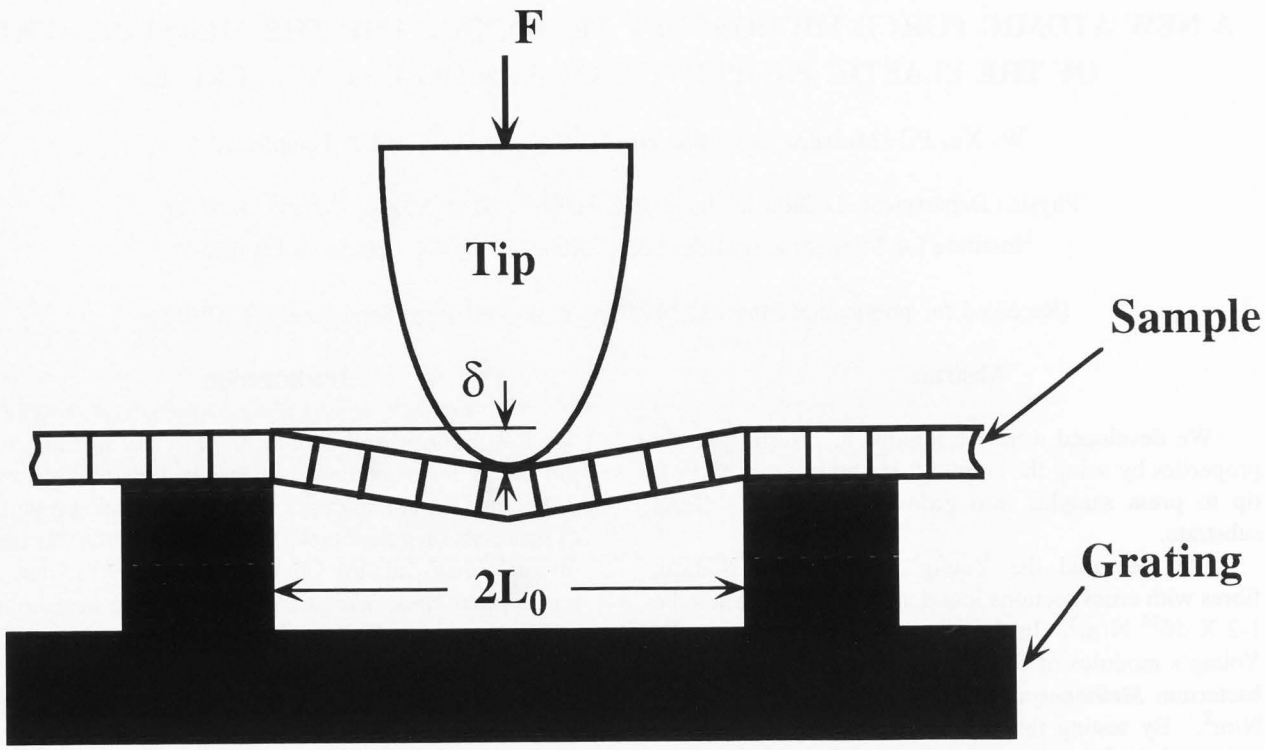

Figure 1. Illustration of the arrangement of the grating, sample, and AFM tip for the elasticity measurement. The force, F, causes a depression, δ, at the centre of the suspended sample. The sample might stretch as shown, or the pressure of the tip might indent the material and make it conform to the tip shape. Except for the depth of the groove, the diagram is approximately to scale for our measurements of sheath.

---

nique was only suitable for long, narrow materials. We now use a specially prepared GaAs "grating" with ion milled grooves on the surface (fabricated by the Institute for Microstructural Sciences at the National Research Council, Ottawa, Canada). These grooves were 300 nm, 500 nm, and 700 nm wide, many micrometers long, and 300 nm deep. The grooves had sufficiently sharp edges to allow accurate measurements of the span lengths, and the assortment of widths made it possible to compare results from different span lengths.

Our technique is illustrated schematically in Figure 1. The material of interest was deposited on the grating, and some of it would span one or more of the gaps, effectively forming a beam or plate supported over a gap in the grating. The AFM tip was then placed on the centre of the span and the deflection measured as the imaging force increased.

First, an area was scanned at minimum imaging force to locate the material and measure its dimensions. Second, the tip was moved to rest near the centre of the span over the gap. Third, the imaging force was increased, and the deflection of the material was measured by monitoring the z-piezo displacement. The resulting displacement versus force data, combined with the dimensions, was used to determine the elastic properties.

We used an interferometer type AFM (Mulhern *et al.*, 1991) with commercial Si tip cantilevers (force constants = 0.16 to 0.76 N/m) for all our measurements. The force applied to a sample was controlled by altering the reference setting of the feedback loop, which altered the operating point on the interference fringe. Changing the operating point on the fringe required changing the interferometer gap, which in turn meant bending the cantilever holding the tip. The force applied to the sample was calculated from the cantilever force constant and the change in cantilever deflection. The force constant was determined from the cantilever resonance frequency. The movement of the z-piezo was the sum of the deflection of the material under the tip and the change in the interferometer gap. Displacement versus force curves were measured for the tip in contact with the bare GaAs substrate, and after allowing for the indentation of the GaAs substrate, this served as a measure of the change in interferometer gap under different

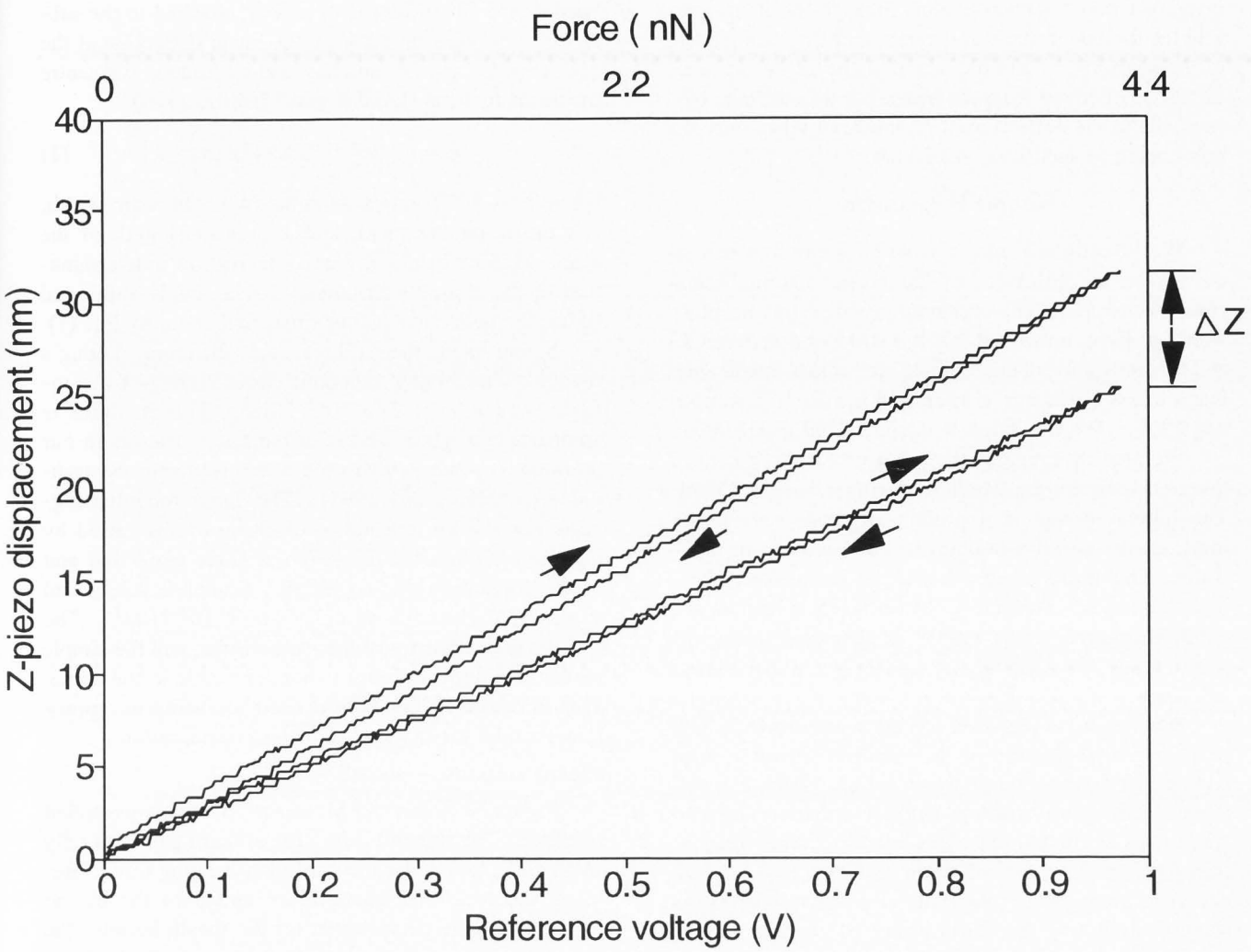

Figure 2. Plot of the displacement of the z-piezo versus the applied force as determined by the reference voltage. First, a baseline is established by measuring the piezo displacement over the bare substrate. The upper curves were measured with the tip pressing on the centre of a β-chitin fibre span. The displacement of the fibre, δ, is the difference between the two sets of curves, Δz.

---

forces. The deflection of the material under investigation was the difference between the z-piezo displacement over the material at a given force and the indentation-corrected displacement over the GaAs at the same force. In practice, the GaAs indentation correction [for the appropriate formula see Weisenhorn *et al.* (1993a)] for the 20 nm tip radius in our experiments was at most 1.8 nm at the largest forces employed. The elastic properties of the biological material were obtained by measuring changes in the cantilever deflection as the loading forces were varied. This meant that, although capillary forces between tip and biological material can greatly increase the force the tip exerts on the top surface of the material, their effect on the overall deflection of the suspended material should be minor.

Figure 2 shows a z-piezo displacement versus force curve for chitin. The lower curve is the deflection due to force on the bare substrate. The results for increasing and decreasing force are indistinguishable, indicating that the GaAs responded elastically over the force range used. The upper curves in Figure 2 are the z-piezo displacements over the chitin when pressing at the centre of the span. These curves show a slight hysteresis, although the response is approximately elastic. The displacement, Δz, is the deflection of the fibre.

An alternative measurement technique can be used if the suspended member has an intrinsic sag and the response of the system to an applied force is non-linear. Complete images of the material under consideration and the supporting grating can be measured at different

imaging forces. Cross-sections through the images reveal the total depression at the center of the span relative to the supports. Note the actual shape of the material cannot be obtained from the image because the data corresponds to the deflection of the material when only the point being imaged was under load.

Sample Preparation

We investigated pure crystalline β-chitin, a natural polysaccharide, produced by the marine diatom *Thalassiosira fluviatilis*. The organism produces this in spines $\sim$60 μm long, up to 100-200 nm wide, and between 50 and 70 nm thick. These spines are in turn made from macrofibres 20-30 nm wide and 18 nm thick (Dweltz *et al.*, 1968). We measured both spines and macrofibres.

We also investigated the outer protective sheath of the archaeobacterium *Methanospirillum hungatei* GP1. The tubular sheath is a protein structure several μm long, almost 440 nm in diameter, and with 9 nm thick walls. The sheath is an assembly of hoop-like components discussed extensively elsewhere (Southam *et al.*, 1993; Blackford *et al.*, 1994). In this experiment, the sheath tubes are collapsed flat, and have a total thickness of 18 nm.

Samples were prepared for the microscope by first preparing a suspension of the material in water, then adding a drop of the liquid to a substrate. Earlier experiments with optical gratings suggested that surface tension forces could pull the fibres into the grating troughs, therefore, the first tests of chitin on GaAs used a freeze drying technique to dry the sample. Later tests on GaAs showed air drying the chitin produced equally suitable samples as freeze drying. The sheath material was deposited using air drying.

Results, Modelling, and Analysis

The AFM measures the vertical force and displacement, but the tension and strain in the material are the relevant parameters to determining the elastic constants. The measured data are converted to the important parameters by modelling such key aspects as the relative dimensions of the span, the boundary conditions, and the anisotropy of the material, and using these in appropriate equations from standard elasticity theory.

Beam bending - Chitin

Figure 3 is an image of a chitin fibre on the GaAs grating. The fibre has a rectangular cross-section of 150 nm x 60 nm, and the longest suspended section is about 1000 nm long.

The rigidity of chitin and the small deflection relative to the length of the span suggested that a beam bending model was appropriate. The ends of the beam were considered fixed rather than simply supported because the fibres appear to be well attached to the substrate. The relation between the beam deflection at the centre of the span, δ, and the loading force at the centre of the span, F, is (Landau and Lifshitz, 1970)

$$\delta = (1/16)\ (F/Ew)\ (2L_o/t)^3 \qquad (1)$$

where E is the Young's modulus, w is the beam width, t is the beam thickness, and $2L_o$ is the length of the span. Measurements of F and δ then allow a determination of the Young's modulus. For a simply supported beam, the deflection is four times that given by Eq. (1).

Spines and macrofibres had different Young's moduli. The Young's modulus for a variety of macrofibres was E = 1-2 X 10^{11} N/m^2. This modulus is comparable to glass, and is of the same order as in our preliminary study which used a less sophisticated technique (Jericho *et al.*, 1993). The above modulus suggests that the tip indentation of chitin beams varied by less than 0.1 nm for the range of force employed and beam indentation was neglected. Complete spines had a measured modulus of only $\sim$5 X 10^9 N/m^2. The spines are composites of the macrofibres, and the simple model of a uniform beam is not applicable to the spine. This underscores the critical need for using an appropriate model for the system under consideration.

Elastic response - Sheath

Figure 4 is an AFM image of two suspended sheathes. The sheath bridges the 300 nm gap with only small deflection under the minimum imaging force. Relating the measured quantities F and δ to the elastic modulus is more complicated for the sheath because the variation of the strain field with distance from the tip is two dimensional, and some simplifying assumptions are not valid because only two of the four edges of the sheet are clamped. We measured the sheath using both the techniques described above.

We modelled the system using three assumptions. First, we knew from earlier STM and AFM imaging that the sheath material has very little bending rigidity (Southam *et al.*, 1993; Blackford *et al.*, 1994). Therefore, only tensile forces in the sheath need to be considered. Second, the strain on a thin membrane clamped at two ends and loaded in the centre is taken primarily in the area between the clamped ends and the indentor, and the free edges take minimal strain (macroscopically, this can be illustrated by clamping the opposite ends of a piece of plastic wrap and putting a small weight on the centre). We considered the strain on the trapezoidal regions bounded by the ends of the sheath on the substrate, w_o, and a length equal to the diameter of the AFM tip, w_t. Third, any curvature in the trapezoidal areas was ignored. The relation between deflection, force, and Young's modulus for the trapezoidal model is

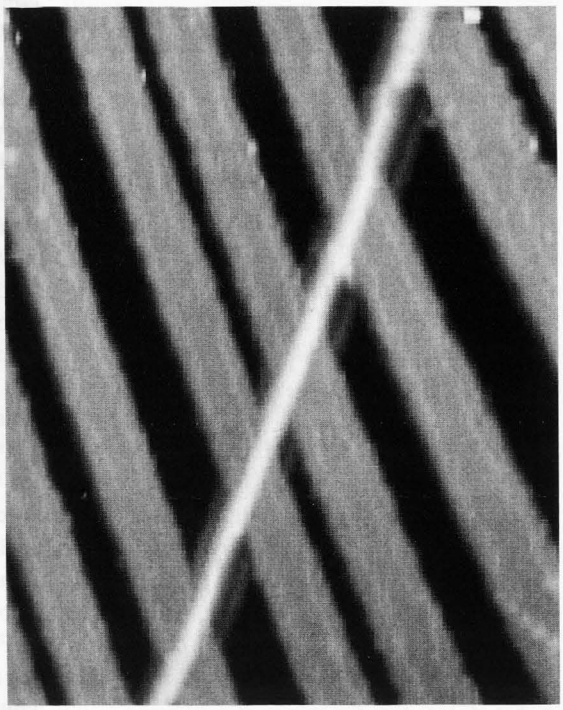

Figure 3. Top view image of a β-chitin fibre supported by the GaAs grating. Scan size is 5700 nm by 6850 nm. The grating gaps are 700 nm, 500 nm, and 300 nm wide and 300 nm deep. The spine has a cross-section of 150 nm X 60 nm.

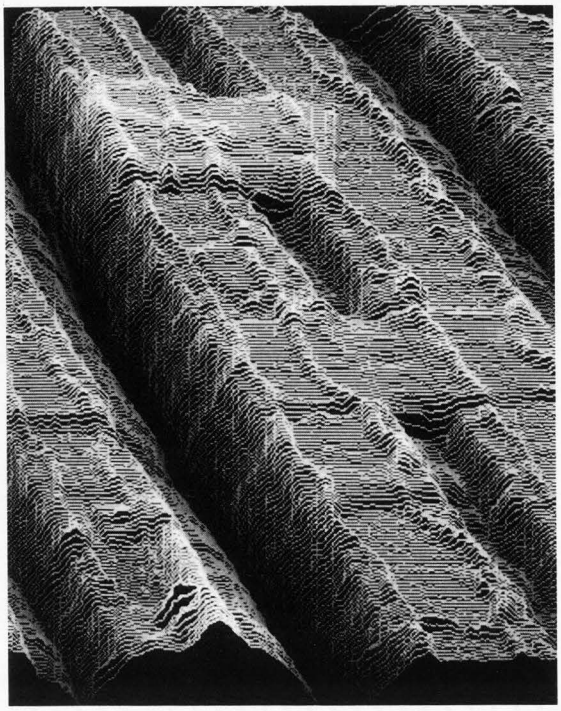

Figure 4. Example of two *M. hungatei* sheathes suspended over a 300 nm wide gap. Scan size is 2900 nm by 3800 nm. Image reconstruction is a view 20° from the vertical.

$$F \approx w_{eff}\, tE\delta\, (\delta^2 - \delta^2_o)\, (1/L_o)^3 \qquad (2)$$

where F is the loading force, w_{eff} is the effective sheath width, t is the thickness, E is the Young's modulus, and $2L_o$ is the width of the suspended region. The sag at the centre of the sheath with no loading or imaging force is δ_o, and the δ is the deflection at the applied force. The effective width, w_{eff}, is

$$w_{eff} = (w_o - w_t) \,/\, \ln (w_o/w_t) \qquad (3)$$

A plot of F/δ versus δ^2 was used to analyze the data. Capillary forces can bring tip and sample surface prematurely together when the tip approaches and could thus affect δ_o. In our experiment, however, the intercept is obtained from the zero force intercept of the F/δ vs δ^2 plot and δ_o is not affected by additional capillary forces. The tip radius was estimated from the tip broadening effects at the edges of the grating and the sheath edges. For a sheath width of w_o = 650 nm and a radius of curvature for the tip of 20 nm, then w_{eff} is 220 nm. Measurements on several sheath bridges gave δ_o values ranging from 7 nm to 9 nm and the corresponding Young's moduli ranged from 1 to 3 X 10^{10} N/m^2. The model gave very consistent results for a variety of sheathes, forces, and gaps. The above analysis of the data did not allow for slippage of the sheath over the grating supports and between the two layers of the collapsed sheath cylinder. In the analysis only those results were considered for which a cycling of the loading force from small to large and back to small gave reproducible deflection results. This was the case for most sheath bridges examined. The interferometer method of detecting the cantilever deflection unfortunately precluded a continuous variation of the loading force over a large range (i.e., several fringes) and hence made it impossible to obtain a continuous force versus deflection curve through the elastic limit.

Plastic deformation - Sheath

The plastic deformation of the sheath gives information on the ultimate strength of the material. Loading forces in excess of $F_c \approx 1 \text{ X } 10^{-7}$ N (corresponding to a $\delta_c \approx 20$ nm, which was approximately the thickness of the sheath bridge) caused irreversible deformation. Figure 5a shows a 50 nm diameter deformation, and Figure 5b is a cross-section through the deformation. The depression is deeper than the thickness of the

sheath, but since the imaging tip is comparable in size to the depression it made, it cannot distinguish between a true hole in which the sheath material was punched through or a 20 nm deep plastic deformation with sheath material still covering the bottom of the depression. Tip forces in excess of 1 X 10^{-7} N formed holes with diameters up to 100 nm in the suspended region while leaving the immediate vicinity of the hole area undamaged.

Yield information can be used to determine absolute physical limits on internal pressures. Relating the critical force, F_c, to the maximum tension in the sheath requires modelling the response of the sheath in the immediate vicinity of the tip. We analyzed sheathes that were deposited with the constituent hoops lying parallel to the gap. Transmission electron microscopy (TEM), scanning tunneling microscopy (STM) and AFM images suggest that the sheath tends to fracture along the boundaries between the hoops that make up the tube of the sheath (Southam *et al.*, 1993). Two models estimated the maximum and minimum value of the critical tension from the critical force.

If the strained regions of the sheath do not curve between the edge of the gap and the tip, as pictured in Figure 1, then the critical tension, T_c, is 3.6 X 10^{-7} N. The length of hoop-hoop bond being stretched by this tension could be as small as ~40 nm (the width of the tip if the tip is directly over a hoop-hoop bond) or as large as ~80 nm (the width of a trapezoidal region half a hoop size away from the tip). The maximum sustainable tension for the complete bacteria is then 2.9-5.8 X 10^{-6} N. This in turn implies a maximum internal pressure of 190-380 atm (1.9-3.8 x 10^7 N/m^2).

Alternatively, if the sheath under the tip deforms to conform to the tip shape, then the greatest force per unit area is applied over the maximum contact perimeter. In this case, T_c is applied over a larger area, and the corresponding maximum pressure is lower. If we assume a 45° angle between T_c and F_c, then the maximum pressure is ~50 atm (5 x 10^6 N/m^2). Because the sheath does not tend to compress significantly under load, we believe the true maximum internal pressure to be at least 100 atm (1 x 10^7 N/m^2).

Discussion

Not discussed above are the difficulties involved in preparing suitable materials for this (or any other) AFM technique. Each new material being studied has unique properties and preparation techniques must be developed for each one. The material of interest must be removed from other biological material present and reduced to sub-micron size. The purification of the sample is particularly critical because contaminants may co-deposit with the material of interest. Also, the dimensions of the sample, the width of the gaps, and the force constant of the lever must all be matched to allow for a suitable span of material and a depression into the gap.

The overall accuracy of the method for determining the elastic constant of a biological material will depend on the type of material investigated and the extent to which the various assumptions apply. For fibers with rigidity, such as the crystalline beta-chitin, the beam formula should apply and the main source of error would come through the assumptions about the boundary conditions. For fibers with little or no rigidity, depression of the fiber into the gap should be largely a result of fiber stretch (provided no slip occurs at the supports and provided the tip is sufficiently blunt that fiber indentation can be neglected) and we expect Eq. (2) to give a reasonable representation of the depression distance as a function of load. For membranes that are narrow compared to the gap width, the force per unit length in the membrane as a consequence of an applied load by the tip is approximately constant along a line parallel to the support edge and Eq. (3) should be applicable. For a membrane that is wide compared to the gap width, such as the sheath in this study, the force per unit length is not strictly constant. An effective width can still be defined, however, and is about 30% smaller than the value used above. A detailed discussion of this more general case will be presented elsewhere. The value of the elastic modulus derived from the data depends on the choice for the contact radius between tip and membrane. Depending on how the membrane deforms around the tip, the contact radius may be comparable to the tip radius in an extreme case. The effective width only depends logarithmically on the contact radius, however, and uncertainties in the contact radius together with the inevitable variation from sample to sample are expected to affect the calculation of Young's moduli by at most a factor of 2-3. Although this represents a large uncertainty, the elastic properties of biological material at the nanometer scale are difficult to obtain and determination of the modulus to an order of magnitude is often of interest. Weisenhorn *et al.* (1993b) also reported large variations (a factor of four) of the elastic modulus for rubber and cartilage obtained with the indentation method.

This new technique for measuring elasticity by bending or stretching a material into a microscopic gap could be applied to smaller structures if smaller width grating grooves can be manufactured. In principle, the technique should be able to provide information on the bulk elastic properties of biological components and the method compliments the simple indentation technique (Weisenhorn *et al.*, 1993a). The technique can be extended to measuring forces under an aqueous solution containing the buffer salts present in a living organism,

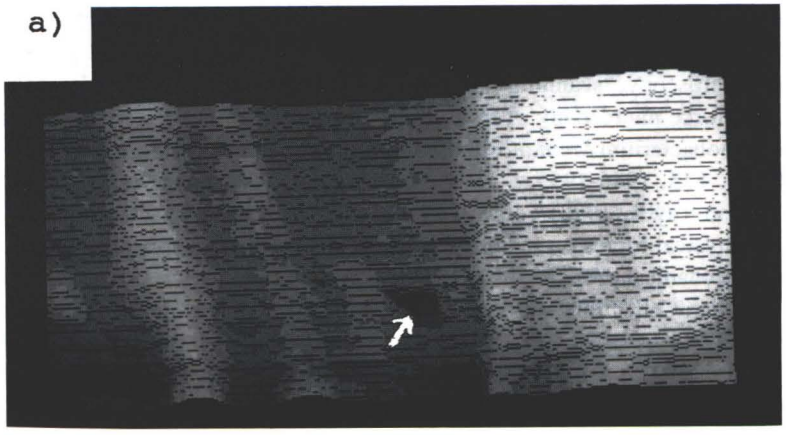

Figure 5a. By raising the tip force to 1 X 10^{-7} N, a 50 nm permanent deformation was created in the sheath (see arrow). This image was measured after returning the imaging force to a minimum. Scan size is 990 nm by 540 nm. Image reconstruction is a view 20° from the vertical.

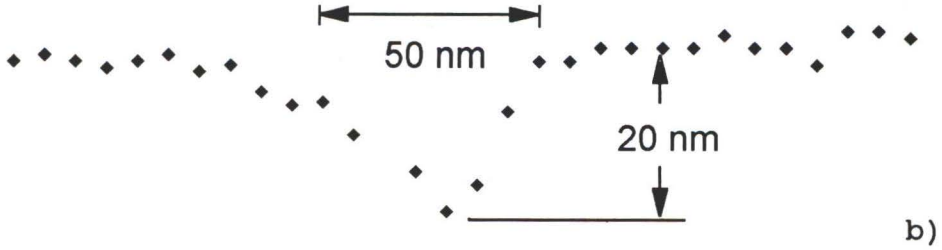

Figure 5b. Cross-section through the depression reveals that the depth is greater than the collapsed sheath cylinder.

thereby opening the possibility of measuring biological properties *in situ*.

List of Symbols

δ	deflection of the material at the centre of the span (nm)
δ_c	maximum deflection at the elastic limit (nm)
δ_o	sag at the centre of the sheath with no loading force (nm)
E	Young's modulus (N/m^2)
F	force (N)
F_c	critical force for the sheath at the elastic limit (N)
L_o	half length of the span (nm)
t	thickness of the material (nm)
T_c	critical tension for the sheath at the elastic limit (N)
w	beam width (nm)
w_{eff}	effective sheath width (nm)
w_o	width of the trapezoid at the grating end (nm)
w_t	width of the trapezoid at the tip end (nm)
Δz	net z-piezo displacement due to the deflection of the material (nm)

Acknowledgements

This work was partially supported by operating grants from the Natural Sciences and Engineering Research Council of Canada. We thank L. Fritz of the National Research Council of Canada Institute for Marine Biosciences who supplied the chitin, and T.J. Beveridge and M. Firtel of the University of Guelph who supplied the *M. hungatei* sheath.

References

Blackford BL, Xu W, Jericho MH, Mulhern PJ, Firtel M, Beveridge TJ (1994) Direct observation by scanning tunneling microscopy of the two-dimensional lattice structure of the S-layer sheath of the archaeobacterium *Methanospirillum hungatei* GP1. Scanning Microsc. **8**, this issue.

Dweltz NE, Colvin JR, McInnes AG, (1968) Studies on chitan (β-(1→4)-linked 2-acetamido-2-deoxy-D-flucan) fibers of the diatom *Thalassiosira fluviatilis*, Hustedt. III. The structure of chitan from X-ray diffraction and electron microscope observations. Can. J. Chem. **46**, 1513-1521.

Evans EA, Waugh R, Melnik L (1976) Elastic area compressibility modulud of red cell membrane. Biophys, J. **16**, 585-595.

Jericho MH, Mulhern PJ, Xu W, Blackford BL, Fritz L (1993) SFM and STM imaging of β-chitin. In: Scanning Probe Microscopies II, SPIE Proc. **1855**, 48-56.

Landau LD, Lifshitz EM (1970) Theory of elasticity. Pergamon Press, New York. pp. 75-100.

Mulhern PJ, Hubbard T, Arnold CS, Blackford BL, Jericho MJ (1991) A scanning force microscope with a fiber-optic-interferometer displacement sensor. Rev. Sci. Instrum. **62**, 1280-1284.

Southam G, Firtel M, Blackford BL, Jericho MH, Xu, W, Mulhern PJ, Beveridge TJ (1993) Transmission electron microscopy, scanning tunneling microscopy, and atomic force microscopy of the cell envelope layers of the archaeobacterium *Methanospirillum hungatei* GP1. J. Bacteriol. **175**, 1946-1955.

Tran-Son-Tay R (1993) Techniques for studying the effects of physical forces on mammalian cells and measuring cell mechanical properties. In: Physical Forces and the Mammalian Cell. Frangos JA (ed.). Academic Press, San Diego, CA. pp. 1-59.

Weisenhorn AL, Kasas S, Solletti J-M, Khorsandi M, Gotzos V, Roemer DU, Lorenzi GP (1993a) Deformation observed on soft surfaces with an AFM. In: Scanning Probe Microscopies II, SPIE Proc. **1855**, 26-34.

Weisenhorn AL, Khorsandi M, Kasas S, Gotzos V, Butt H (1993b) Deformation and height anomaly of soft surfaces studied with an AFM. Nanotechnology, **4**, 106-113.

Discussion with Reviewers

D.C. Dahn: If you compare images before and after the hole is made, is there any evidence for irreversible damage in the region immediately around the hole in Figure 5? The work done by the tip in deforming the sheath could be calculated; would it be possible to equate this to the energy required to break hoop-hoop bonds around the hole, or is there significant additional deformation produced?

Authors: As stated in the text, tip forces in excess of 1×10^{-7} N formed holes with diameters up to 100 nm in the suspended region while leaving the immediate vicinity of the hole area undamaged. The maximum force, and hence the maximum local stretch of the membrane, should, in principle, permit an estimate of the strength of the bonds that hold the membrane together. In practice, this estimate depends on the length of the membrane over which bonds are broken and on the microstructure of the membrane in the vicinity of the break. One model that might be explored is one in which the hoops are assumed to be unstretchable and all the elastic energy is put into the hoop-hoop bonds.

V. Moy: Two models were used on the analysis of the different samples. With respect to the specimens measured in this study, are there significant variation in the Young's modulus between the models?

Authors: The two models are fundamentally different. The formula used for the chitin fibres is the standard formula for a beam that has substantial bending rigidity. The model for the sheath, on the other hand, is based on the assumption that the sheath has negligible bending rigidity and therefore the deflection of the sheath is due to pure stretching of the material in the sheath plane. Which formula is appropriate therefore depends on the properties of the material to be investigated. If a biological fibre overhangs an edge without substantial drooping (like a pencil that overhangs the edge of a table) then the beam formula should be appropriate. If, on the other hand, the fibre has no rigidity and molds itself around the edge (like a string) then the stretch formula should be appropriate. The Young's moduli between two models differ from each other by 1-2 orders of magnitude for the two specimens measured in this study.

D.A. Chernoff: Is the beam deflection method likely to be more reliable than the indentation method? Please discuss the role of model assumptions in the interpretation of results in these two geometries.

Authors: The indentation method is suitable for materials which are relatively large and thick such that the indentation formula apply. For hard, or relatively thin samples, such as a membrane, the observed indentation is either very small or may also be affected by indentation of the substrate. Our method on the other hand can produce relatively large deflections without having the substrate effect involved. Furthermore, we believe that, for biological materials, the deflection measurement by bending or stretching the material provides data which is more relevant to the bulk elastic properties of the material than the measurement of small surface indentation. The role of the model assumptions in the interpretation of results is fully explained in the text.